Theoretical study of phenolic antioxidants properties in reaction with oxygen-centered radicals

ARTICLE *in* JOURNAL OF MOLECULAR STRUCTURE THEOCHEM · NOVEMBER 2006

Impact Factor: 1.37 · DOI: 10.1016/j.theochem.2006.07.017

1 AUTHOR:

Katarina Nikolic
University of Belgrade
62 PUBLICATIONS **255** CITATIONS

SEE PROFILE

ELSEVIER

Journal of Molecular Structure: THEOCHEM 774 (2006) 95–105

THEO CHEM

www.elsevier.com/locate/theochem

Theoretical study of phenolic antioxidants properties in reaction with oxygen-centered radicals

Katarina M. Nikolic *

Department of Medicinal Chemistry, Pharmacy Faculty, University of Belgrade, Vojvode Stepe 450, 11000 Belgrade, Serbia and Montenegro

Received 23 February 2006; received in revised form 20 July 2006; accepted 20 July 2006
Available online 26 July 2006

Abstract

A dominant transfer mechanism [hydrogen atom transfer (HAT) or proton-coupled electron transfer (PCET)] in the reaction of phenols with certain types of oxygen-centered radicals was selected by examining the conformations, singly occupied molecular orbitals (SOMOs), charge separation and spin density in optimized transition structures (TSs) such as $(CH_3)_3$–C–O_3–$O_2^{\cdot}\cdots H\cdots O_1$–Ar and $(CH_3)_3$–C–$O_2^{\cdot}\cdots H\cdots O_1$–Ar. The change in charge on the hydrogen (ΔH) and the SOMO conformations in the TS $(CH_3)_3$–C–O_3–$O_2^{\cdot}\cdots \mathbf{H}\cdots O_1$–Ar or $(CH_3)_3$–C–$O_2^{\cdot}\cdots \mathbf{H}\cdots O_1$–Ar were used as criteria for determining the dominant H-atom transfer mechanism. Increased electron density on the O_2 and O_3 oxygens in the PCET-TS selectively stabilizes the TS by providing greater binding energy for H^+ transfer. Thus, the (O_2+O_3−O_1) charges, Δ(O_2+O_3−O_1) charges, and (O_2+O_3) spin densities in the PCET-TS were well correlated with the experimental antioxidative activity (k_1). The spin densities on the radical oxygens (O_2+O_3) in the HAT-TS were highly negatively correlated with k_1, while the spin densities on the ring in the HAT-TS showed good positive correlation with k_1 values. In the TS of phenols containing O_7(*para*) in the structure, the spin densities on O_7(*para*) and on the ring were correlated well with k_1. Since the reactivity of phenols with an alkylperoxy radical does not strongly depend on the radical structure, the procedure presented here can be used to estimate phenol reactivity with any alkylperoxy radical (R–O–O$^{\cdot}$).

Keywords: Antioxidant activity; Phenols; Bond dissociation enthalpy; Molecular orbitales; Transition states

1. Introduction

Phenolic antioxidants such as vitamin E, hydroxytyrosol, gallic acid, caffeic acid, chicoric acid, flavonoids and epicatechin are extremely important peroxy radical-trapping agents in human blood plasma and in cells. They inhibit the oxidation of lipids, fats, and proteins (RH) by donation of a phenolic hydrogen atom to the chain-carrying peroxy radical (ROO$^{\cdot}$) [1,2]. The stereoelectronic effects of phenols (Ar–OH) and phenoxyl radicals (Ar–O$^{\cdot}$) are largely responsible for their reactivity with ROO$^{\cdot}$ [3].

The reaction mechanisms by which the hydrogen atom (H$^{\cdot}$) of a phenol (Ar–OH) is transferred to an ROO$^{\cdot}$ radical [Eq. (1)] can be divided into two distinct pathways, hydrogen atom transfer (HAT) and proton-coupled electron transfer (PCET) [4].

$$\mathrm{ROO^{\cdot}} + \mathrm{Ar{-}OH} \xrightarrow{k_1} \mathrm{ROOH} + \mathrm{Ar{-}O^{\cdot}} \quad (1)$$

Effective phenolic antioxidants (Ar–OH) need to react faster than biomolecules (RH) with free radicals to protect the latter from oxidation ($k_1 \gg k_2$) [5,6].

$$\mathrm{ROO^{\cdot}} + \mathrm{RH} \xrightarrow{k_2} \mathrm{ROOH} + \mathrm{R^{\cdot}} \quad (2)$$

The phenoxyl radical (Ar–O$^{\cdot}$) formed can react with another free radical (ROO$^{\cdot}$) or with a new substrate (RH):

$$\mathrm{ROO^{\cdot}} + \mathrm{Ar{-}O^{\cdot}} \rightarrow (\mathrm{Ar{-}O})\mathrm{OOR}\ \text{(fast reaction)} \quad (3)$$

$$\mathrm{Ar{-}O^{\cdot}} + \mathrm{RH} \rightarrow \mathrm{Ar{-}OH} + \mathrm{R^{\cdot}}\ \text{(slow reaction)}\ (k_3 \gg k_4) \quad (4)$$

In fact, the antioxidant (Ar–OH) needs to react faster than the substrate (RH) with the free radical (ROO$^{\cdot}$) ($k_1 \gg k_2$), while the Ar–O$^{\cdot}$ radical formed should react

* Tel.: +357 99 832 183; fax: +357 25 581 240.
E-mail address: katarina.nikolich@gmail.com

0166-1280/$ - see front matter © 2006 Elsevier B.V. All rights reserved.
doi:10.1016/j.theochem.2006.07.017

rapidly with another ROO$^{\bullet}$ radical [Eq. (3)] and slowly with a new substrate RH [Eq. (4)] or another Ar–O$^{\bullet}$ radical [Eq. (5)].

$$\text{Ar–O}^{\bullet} + \text{Ar–O}^{\bullet} \rightarrow \text{ nonradical products } (k_3 \gg k_5) \quad (5)$$

In the HAT pathway, a whole hydrogen atom (H$^{\bullet}$) is abstracted from a phenol (Ar–OH) by the oxygen of a radical (RO**O**$^{\bullet}$) using the same sets of orbitals [Eq. (1)] [4]. Thus, it was logical to examine the bond dissociation enthalpy (BDE) of the of the phenol bond [BDE(Ar–OH)^{gas}] [7] as a good primary indicator of phenol reactivity via HAT [Eq. (6)].

$$\text{Ar–O–H} \rightarrow \text{Ar–O}^{\bullet} + \text{H}^{\bullet} \quad (6)$$

Because the energy of molecular orbitals and the geometry of phenols and the corresponding phenoxyl radicals may influence the BDE(Ar–OH)^{gas} values, the highest occupied molecular orbital of the phenols, HOMO(Ar–OH), and the singly occupied molecular orbital of the phenoxyl radicals, SOMO(Ar–O$^{\bullet}$), were also examined [3,7].

In the PCET mechanism, the hydrogen atom (H$^{\bullet}$) of Ar–OH is transferred as a proton (H^+) and an electron to the radical oxygen (RO**O**$^{\bullet}$) using different sets of orbitals. This means that the electron is transferred from the phenol oxygen (Ar–**O**–H) to the radical oxygen (RO–**O**$^{\bullet}$), while the hydrogen is moved as a H^+ ion [4]. It is clear, however, that for estimation of phenol PCET reactivity, the ionization potential [IP(Ar–OH)] is of particular importance [5,8]. Previously reported linear relationship between phenol HOMO(Ar–OH) energies and the experimental/calculated IP values [8] pointed to the HOMO(Ar–OH) parameter as an indicator of phenol PCET reactivity. In addition, molecular orbitals of the ArO radicals generated, described by SOMO(Ar–O$^{\bullet}$), are expected to have an influence on phenol reactivity via PCET [7].

In fact, both HAT and PCET mechanisms must always occur in parallel, but at different rates.

The net result in the HAT and in the PCET pathways is the same:

$$\text{ROO}^{\bullet} + \text{Ar–OH} \xrightarrow{k_1} \text{ROOH} + \text{Ar–O}^{\bullet}.$$

Thus, it was logical to examine the influence of the HOMO(Ar–OH) and SOMO(Ar–O$^{\bullet}$) energies on the antioxidative characteristics of phenols.

The k_1 values for phenolic antioxidants also depend on the electronic effects of the ring substituents [9], on the steric effects of the ring substituents [10], on intermolecular hydrogen-bonding (HB) interactions between the reactive center and nearby functional groups [11,12], and on the strength of HB interactions between the phenol and the solvent (S) [13,14]. Because the initial H transfer process between the phenol and the oxygen-centered radical requires HB formation with the abstracting radical, only phenols that are not hydrogen-bonded to the solvent molecules are able to react with the free radicals [14].

Therefore, it is necessary to start any analysis from the interaction between the phenol and the solvent (Ar–OH$\cdots$S), and then to continue with examination of the H transfer process between the phenol and the oxygen-centered radical.

The Ar–OH$\cdots$S hydrogen bond can be estimated by evaluating the free energy of the interaction between phenol, a HB donor (HBD) molecule, and the HB acceptor (HBA) solvent using the α_2^H and β_2^H Abraham scale [15,16].

The equilibrium constant (K_1) relative to the interaction between a donor Ar–OH (α_2^H) and an acceptor S (β_2^H) is given by [15,16]:

$$\text{Ar–OH} + \text{S} \overset{K1}{\rightleftharpoons} \text{Ar–OH}\cdots\text{S} \quad (7)$$

$$\log K^1 = 7.354\ \alpha_2^H\ \beta_2^H - 1.094 \quad (8)$$

Solvents capable of both accepting and donating HBs, such as water ($\alpha_2^H = 0.35$, $\beta_2^H = 0.38$), methanol ($\alpha_2^H = 0.41$, $\beta_2^H = 0.37$) and *t*-butyl alcohol ($\alpha_2^H = 0.32$, $\beta_2^H = 0.49$) [15–17], can either enhance or decrease the rate of H transfer between the phenol and the oxygen-centered radical (k_1 value). The overall effect depends on which of the redox couple phenol/phenoxyl radical is better stabilized by the solvent [17].

In the present correlation study, k_1 values were obtained in very non-polar solvents such as styrene and CCl_4 [3,4], so the quantum chemical calculations were performed for the gas phase.

The main objectives of the investigation were to develop a method for detection of the dominant H-atom transfer mechanism (i.e., that with the faster rate) and to select parameters able to predict total antioxidant activity (k_1) of phenols in reaction with particular oxygen-centered radicals.

To select the main H-atom transfer pathway for particular phenols and radicals, the conformations, molecular orbitals, charge separation, and spin density were examined in the transition structures (TSs) of complexes between phenols and oxygen-centered radicals such as $(CH_3)_3$–C–O–O$^{\bullet}\cdots$H$\cdots$O–Ar and $(CH_3)_3$–C–O$^{\bullet}\cdots$H$\cdots$O–Ar.

The first group of phenolic antioxidants were examined in TSs with the *tert*-butyl-peroxy radical $(CH_3)_3$–COO$^{\bullet}\cdots$H$\cdots$O–Ar and compared with the rate constant measured for H-atom abstraction by the radical (k_1 value) [3,18,19].

In the second group of phenolic antioxidants, TSs with the *tert*-butyloxy radical $(CH_3)_3$–CO$^{\bullet}$ were similarly examined [14].

2. Materials and methods

The calculation presented here was performed using CS MOPAC Pro 2000 Version 7.0.0 program [20] and CS Gaussian 98 program [21] with Becke's three-parameter hybrid functional method (B3LYP/6-31G (d,p)) [22,23].

The BDE calculation for major families of phenolic antioxidants (BDE(Ar–OH)^{gas}) has been described in a number of recent publications [24–28]:

$$BDE(ArO–H) = E(elec)_{ArO\cdot} + ZPE_{(s)ArO\cdot} + E(elec)_{H\cdot} - E(elec)_{ArOH} - ZPE_{s\ ArOH} + 5/2RT$$

$$BDE(ArO–H) = E(elec)_{ArO\cdot} + ZPE_{(s)ArO\cdot} + E(elec)_{H\cdot} - E(elec)_{ArOH} - ZPE_{(s)ArOH} + 1.4812\ kcal/mol$$

E(*elec*) – Electronic energy, ZPE – Zero-Point Energy
Scaled Zero-Piont Energy: $ZPE_{(s)} = ZPE{\cdot}0.947$ [23]
Electronic energy of hydrogen radical: $E(elec)_{H\cdot} = -313.96475$ kcal/mol

The geometries of the phenols (ArO–H) and phenoxyl radicals (Ar–O·) were optimized using the semiempirical AM1 (Austin Model 1) method [29,30]. Comparison of the AM1 geometries with known experimental values and other reference data for phenol and phenoxyl radical [27,31–34] shows that the AM1 geometries are sufficiently accurate for our purpose (Supplementary Tables 1 and 2). Vibrational frequencies and zero-point energy (ZPE) were determined using the AM1 method and than scaled by a factor 0.947 to obtain the scaled zero-point energy ($ZPE_{(S)}$) and vibrational contribution to the enthalpy [27].

The electronic energies, E(*elec*), were obtained by density functional theory (DFT) using the B3LYP/6-31G (d,p) basis set [27,28]. Self-consistent field (SCF) convergence criteria were used with the DFT energies calculations of the models. For the phenoxyl radicals, calculation of the electronic energies used the *Restricted Open-Shell* wave function in the B3LYP/6-31G (d,p) basis set [(RO)B3LYP/6-31G(d,p)^{gas}] [28].

The $BDE(C_6H_5–OH)^{gas}$ value of 86.03 kcal mol^{-1}, using the selected AM1/AM1/B3LYP/6-31G (d,p) methods for geometry/ZPE/E(*elec*) calculation, was very close to the experimentally measured $BDE(C_6H_5–OH)^{gas}$ result of 86.7 ± 0.7 kcal mol^{-1} [35–37] (Supplementary Table 3).

In addition, the molecular surfaces of the phenols and phenoxyl radicals examined were calculated using the B3LYP/6-31G (d,p)^{gas} and (RO)B3LYP/6-31G(d,p)^{gas} basis sets, respectively.

To investigate the mechanisms of hydrogen atom transfer from phenolic antioxidants (Ar–OH) to oxygen-centered radicals (ROO· or RO·), the TSs (Ar–O···H···O–O–R or Ar–O···H···O–R) were characterized using the *Unrestricted Open-Shell* wave function in the B3LYP/6-31G (d,p) basis set [(U)B3LYP/6-31G(d,p)^{gas}] [4]. TS optimization was started with the MOPAC/AM1/Open Shell method, with selection of a TS conformation in which the H atom is almost equidistant (1.1–1.2 Å) [4] from the O_1 and O_2 oxygens (Ar–O_1···**H**···O_2–O_3–R or Ar–O_1···**H**···O_2–R). The TS chosen in the MOPAC/AM1/Open Shell method was further optimized by the (U)B3LYP/6-31G(d,p)^{gas} method [4]. This approach minimized the computation time required for the (U)B3LYP/6-31G(d,p)^{gas} method. The (U)B3LYP/6-31G(d,p)^{gas}-optimized transition structures were characterized by frequency calculations showing a single imaginary.

Furthermore, molecular surfaces, partial atomic charges, and spin densities of the optimized TSs were calculated using the (U)B3LYP/6-31G (d,p) basis set, with ChelpG population analysis [4,38]. Previous theoretical study of hydrogen atom exchange reactions between phenol and oxygen-centered radical [4] were calculated (U)B3LYP/6-31G (d,p) partial atomic charges of reactants and TSs with Natural Atomic Population (NAP) and ChelpG population analysis. The NPA results were qualitatively similar to the results of the ChelpG population analyses [4].

Because of the complexity of the quantum chemical computations for the bulky tocopherol TSs, molecular models of the tocopherols, with a methyl group bonded in position-2 of the chromanol instead of an aliphatic side chain, were used [27]. The substituted aliphatic chain does not have a significant influence on the antioxidative activity of tocopherols [27].

3. Results

The AM1/AM1/B3LYP/6-31G (d,p) procedure was used to calculate $BDE(Ar–OH)^{gas}$ for the phenolic antioxidants [39]. The theoretical $\Delta BDE(Ar–OH)^{gas}$ values for the phenols derived by the AM1/AM1/B3LYP/6-31G (d,p) method using a calculated $BDE(C_6H_5–OH)^{gas}$ value of 86.03 kcal mol^{-1} were in good agreement ($r = 0.968$)

Table 1
Experimentally measured $\Delta BDE\ (Ar–OH)^{benzene}$ of some phenols [39–41] relative to the experimental $BDE\ (C_6H_5–OH)^{benzene}$ value of 88.3 ± 0.8 kcal/mol [39]

Phenols Ar–OH	$\Delta BDE(Ar–OH)^{benzene}$ experimental (kcal/mol)	$\Delta BDE(Ar–OH)^{gas}$, B3LYP/6-31G (d,p) (kcal/mol)	Difference Δ(ΔBDE) (kcal/mol)
4-Methyl-phenol	−2.1 [39]	−2.0	−0.1
4-(*tert*-Butyl)-phenol	−3.0 [39]	−1.6	−1.4
4-Methyloxy-phenol	−5.5 [39]	−5.7	0.2
2,3,6-Trimethyl-4-methoxy-phenol	−9.1 [39]	−10.3	1.2
2,3,5,6-Tetramethyl-4-methoxy-phenol	−6.4 [39]	−8.2	1.8
4-Amino-phenol	−12.7 [40]	−12.9	0.2
Ia	−10.0 [41]	−12.9	2.9
Correlation-*r*,experm. ΔBDE/theoretical ΔBDE		0.968	

Theoretical $\Delta BDE\ (Ar–OH)^{gas}$ of the phenols derived by AM1/AM1/B3LYP(6-31G (d,p)) method, relative to the calculated $BDE\ (C_6H_5–OH)^{gas}$ value of 86.03 kcal/mol.

with experimentally measured $\Delta BDE(Ar–OH)^{benzene}$ of some phenols [39] using an experimental $BDE(C_6H_5–OH)^{benzene}$ value of 88.3 ± 0.8 kcal mol^{-1} [39–42] (Table 1).

For phenols with single *ortho* and/or *meta* substituents, it was necessary to distinguish between the *away* and *toward* conformations of the OH group relative to the substituent. To avoid the possibility of identifying a local rather than the true energy minimum during AM1 geometry optimization, all optimized structures were scanned visually, multiple starting points were used and the AM1 *Optimization to Transition State* procedure was applied [27].

The previously derived ZPE-corrected enthalpy by DFT calculation and infrared experimental measurements [27] for *o*-methyl-phenol confirmed that the *away* conformer is more stable than *toward* conformer, both in solution and in the vapor phase [27].

The three phenols of the antioxidants examined have a single *ortho* substituent with the *away* conformation in the optimized structures, so we considered the conformations as global minima.

The dominant H-atom transfer mechanism (HAT or PCET) in the reaction of phenols with certain oxygen-centered radicals was selected by examination of optimized TSs, such as $(CH_3)_3–C–O_3–O_2\cdot\cdots H\cdots O_1\cdots Ar$ and $(CH_3)_3–C–O_2\cdot\cdots H\cdots O_1\cdots Ar$ [3,4,38].

Increased electron densities on the O_2 and O_3 oxygens in the PCET-TS selectively stabilize the TS by providing greater binding energy for H^+ transfer [4]. Thus, we examined the charge separations on the oxygens in the optimized TS.

Since delocalization of the unpaired electron in the TS influences its stability and the rate of H-atom transfer [3], we analyzed atomic spin densities in the optimized $(CH_3)_3COO\cdot\cdots H\cdots O–Ar$ structures.

As a check for the presence of spin contamination, most *ab initio* programs calculate the expectation value of the total spin, S^2. If there is no spin contamination this should equal $s(s+1)$, where s equals 1/2 times the number of unpaired electrons. The expectation values of S^2 for the radicals and transition structures studied (S^2: 0.7501–0.7508) were close to the pure doublet value $s(s+1) = 0.75$, so was concluded that the performed open-shell B3LYP calculation created negligible spin contamination [43].

In the first part of the experiment, phenols were divided for convenience into the following classes shown in Fig. 1: tocopherols, α-δ-TOH, 5,7-dimethyl-tocol (DMT), and the related 6-hydroxy-5,7,8-trimethyl-chromanes, group I; phenols, group II; 5-hydroxy-6,7-dimethyl-2,3-dihydrobenzofurans, group III; and 6-hydroxy-4,4,5,7,8-pentamethyl-3,4-dihydrobenzothiopyran.

After calculation of $BDE(Ar–OH)^{gas}$ for the phenols, we computed HOMO(Ar–OH), SOMO(Ar–O$^{\cdot}$), and the partial atomic charges in the optimized models.

The k_1 values used for this examination were measured *in vitro* by the inhibited autoxidation of styrene (IAS) method [3]. The antioxidants were used to inhibit the azo-bis-(isobutyronitrile) (AIBN)-induced thermal autoxidation of styrene at 30 °C. The active oxidant in the IAS method for reaction with the phenols is the poly(peroxysty-

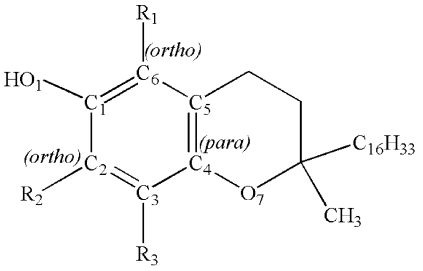

Tocopherols

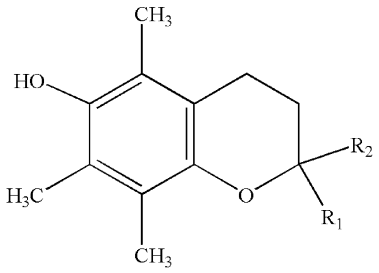

I group

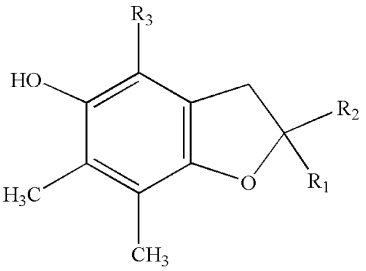

III group

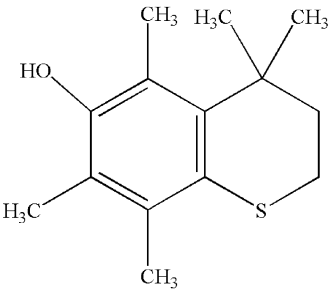

6-hydroxy-4,4,5,7,8-pentamthyl-3,4-dihydrobenzothiopyran

Tocopherols	R_1	R_2	R_3
β-TOH	CH_3	H	CH_3
γ-TOH	H	CH_3	CH_3
δ-TOH	H	H	CH_3
DMT	CH_3	CH_3	H
I group	R_1	R_2	
Ia	CH_3	CH_3	
Ib	H	H	
Ic	CH_3	$C(O)OCH_3$	
Id	CH_3	O CH_3	
III group	R_1	R_2	R_3
IIIa	H	CH_3	CH_3
IIIb	CH_3	CH_3	CH_3
IIIc	CH_3	CH_3	H

Fig. 1. Structures of selected phenolic antioxidants.

ryl)peroxy radical (POO) [3]. The rate of the initial reaction between the phenols and the free radicals [k_1, Eq. (1)] is used as a parameter to describe the antioxidant activity of the phenols analyzed.

The structure of the POO$^{\cdot}$ radical [3] is complicated and bulky for the quantum chemical optimization of the POO$^{\cdot}\cdots$H$\cdots$O–Ar transition structures. Because of fairly strong evidence [18] suggesting that k_1 values do not depend to any great extent on the structure of the alkylperoxy radical (excluding $Cl_3COO^{\cdot}$ [19]), we chose the relatively simple structure of the *tert*-butyl-peroxy radical $(CH_3)_3$–$COO^{\cdot}$ to examine the TSs with selected phenolic antioxidants [$(CH_3)_3COO^{\cdot}\cdots H\cdots O$–Ar] [3]. Furthermore, k_1 values derived using the laser-flash kinetic EPR (LKEPR) method for $(CH_3)_3$–$COO^{\cdot}$ as the active phenol oxidant, were in good agreement with the IAS results [3].

The main difference between HAT and PCET is that the HAT mechanism involves H atom transfer in the TS, while in the PCET mechanism a H^+ ion is transferred from phenol to the radical. Thus, the clearest evidence for the dominant phenol pathway is the change in H-atom charge in the TS compared with the parent phenol.

In fact, a decrease in H-atom charge in the TS relative to the parent phenol is an indicator of a dominant HAT pathway, in which H$^{\cdot}$ is transferred. On the other hand, an increase in H-atom charge in the TS relative to the parent phenol is specific for a dominant PCET mechanism, in which H^+ is transferred [4].

In addition, the SOMO geometries of the O_1 and $O_2^{\cdot}$ atoms in the HAT-TS $(CH_3)_3C$–O_3–$\mathbf{O_2}^{\cdot}\cdots H\cdots O_1$–Ar have almost the same direction as the $O_2^{\cdot}\cdots H\cdots O_1$ bonds, while the SOMO geometries of the O_1 and $O_2^{\cdot}$ atoms in the PCET-TS are nearly orthogonal to the $O_2^{\cdot}\cdots H\cdots O_1$ bonds [4] (Fig. 2).

According to these rules, we classified the phenols into HAT and PCET groups (Tables 2 and 3).

Although the Ia (10^4 $k_1 = 380\ M^{-1}\ s^{-1}$), Ib ($10^4$ $k_1 = 270\ M^{-1}\ s^{-1}$), Ic ($10^4$ $k_1 = 180\ M^{-1}\ s^{-1}$), and Id ($10^4$ $k_1 = 150\ M^{-1}\ s^{-1}$) compounds differ only in substituents far apart from the OH reaction center, the Ic was classified in the HAT, while the other molecules were placed in the PCET group. The main H-atom transfer mechanism for the Ic-TS is detectable from the SOMO (Ic-TS) conformation (Fig. 2) and can be explained by significantly lower HOMO (Ic) energy of −0.190165 hartree, than similarly active Ib and Id molecules, with HOMO (Ib) at −0.186632 hartree and HOMO (Id) energy at −0.184872 hartree.

Since greater electron densities on the O_2 and O_3 oxygens in the PCET-TS selectively stabilize the TS by providing greater binding energy for H^+ transfer [4], the charge separation on oxygens (O_2+O_3−O_1) in all TS were compared with k_1 values. The calculated (O_2+O_3−O_1) values for the PCET-TS were in good negative correlation ($r = -0.865$) with the experimental k_1 values [27] (Table 2).

The charge changes on the O_1, O_2 and O_3 oxygens in the PCET-TS, presented as the Δ(O_2+O_3−O_1) parameter, were relatively highly negatively correlated ($r = -0.882$) with the k_1 values.

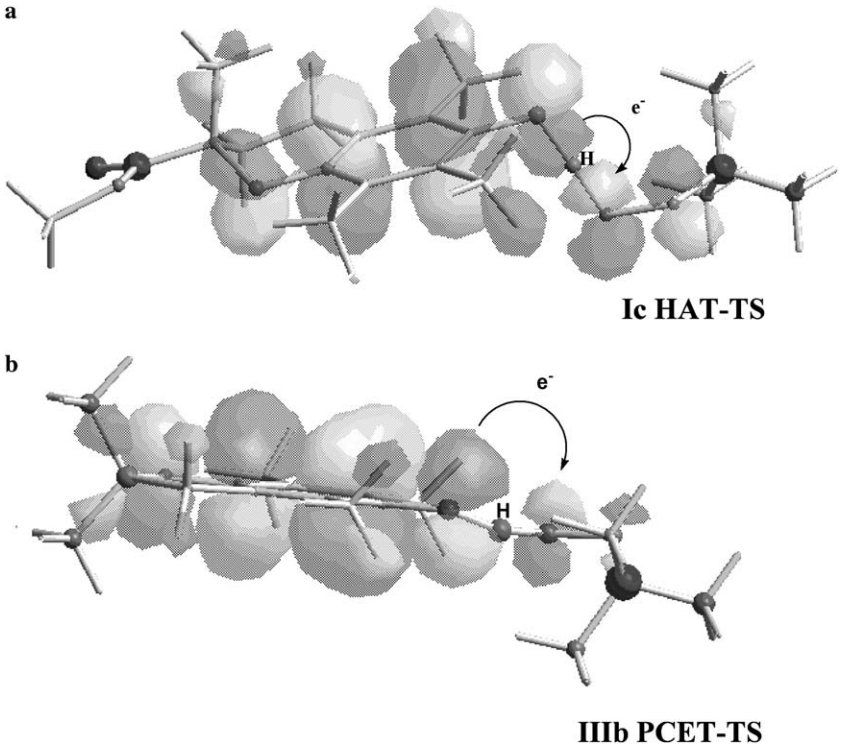

Fig. 2. SOMO conformations of the Ic HAT-TS (a), and the Id PCET-TS (b) with the *tert*-butyl-peroxy-radical ($(CH_3)_3C$–$OO^{\cdot}$).

Table 2
Charge separations in $(CH_3)_3C–O_3–O_2^{\cdot}\cdots H\cdots O_1–Ar$ transition structures computed by (U)B3LYP/6-31G (d,p) basis set with ChelpG population analysis

Compounds	k_1[a]	$O_2+O_3-O_1$ (TS)	H (TS)	Charge (Ar**O**H)	Charge(ArO**H**)	ΔH
HAT						
(*away*) IIIc	320	−0.11675	0.34711	−0.50648	0.38193	−0.03482
Ic	180	−0.18855	0.34278	−0.45616	0.36695	−0.02417
DMT	180	−0.17078	0.36121	−0.48471	0.38753	−0.02632
(*away*) γ-tocopherol[b]	140	−0.08286	0.37218	−0.51447	0.38880	−0.02919
(*away*) β-tocopherol[b]	130	−0.12903	0.36181	−0.52082	0.37922	−0.01741
δ-Tocopherol[b]	44	−0.05069	0.35660	−0.57068	0.40162	−0.04502
Linear correlation factor, *r*		−0.437	−0.451	0.551	−0.501	0.316
PCET						
IIIb	570	−0.27981	0.39717	−0.46719	0.37299	0.02418
IIIa	540	−0.27882	0.38148	−0.48477	0.38115	0.00033
Ia	380	−0.27371	0.50093	−0.45277	0.36374	0.13719
Benzothiopyran derivate	280	−0.22690	0.36513	−0.44555	0.35584	0.00929
Ib	270	−0.20868	0.48855	−0.45884	0.36537	0.12318
Id	150	−0.20526	0.37758	−0.45381	0.36303	0.01455
2,6-Dimethyl-4-methoxy-Ph	94	−0.11249	0.48686	−0.49397	0.39611	0.09075
2,3,5,6-Tetramethyl-4-methoxy-Ph	39	−0.06773	0.45600	−0.44690	0.36367	0.09233
2,4,6-Trimethyl-Ph	8.5	0.08842	0.42674	−0.49864	0.39531	0.03143
2,6-Dimethyl-Ph	2.5	−0.04086	0.44165	−0.51857	0.40704	0.03461
Linear correlation factor, *r*		−0.865	−0.282	0.326	−0.403	−0.142

[a] The k_1 ($M^{-1}\,s^{-1}$) was measured *in vitro* by inhibited autoxidation of styrene (IAS) method [3].
[b] Tocopherol's models.

Table 3
Charge changes in $(CH_3)_3C–O_3–O_2^{\cdot}\cdots H\cdots O_1–Ar$ transition structures relative to the reactants and spin densities in the TS, computed by (U)B3LYP/6-31G (d,p) basis set with ChelpG population analysis

Compounds	HAT		
	k_1[a]	$(C_1+C_2+C_4+C_6+O_7)$ spin	(O_2+O_3) spin
(*away*) IIIc	320	0.54453	0.36706
Ic	180	0.51191	0.39998
DMT	180	0.45567	0.42444
(*away*) γ-tocopherol[b]	140	0.45479	0.44583
(*away*) β-tocopherol[b]	130	0.47497	0.41584
δ-tocopherol[b]	44	0.40886	0.46878
Linear correlation factor, *r*		0.907	−0.925
	PCET		
	k_1[a]	Δ $(O_2+O_3-O_1)$ charge	(O_2+O_3) spin
IIIb	570	−0.43745	0.32235
IIIa	540	−0.45404	0.21973
Ia	380	−0.41693	0.2697
Benzothiopyran derivate	280	−0.36290	0.42322
Ib	270	−0.35797	0.38229
Id	150	−0.34952	0.38762
2,6-Dimethyl-4-methoxy-Ph	94	−0.29691	0.50252
2,3,5,6-Tetramethyl-4-methoxy-Ph	39	−0.20508	0.54617
2,4,6-Trimethyl-Ph	8.5	−0.10067	0.75819
2,6-Dimethyl-Ph	2.5	−0.24988	0.60866
Linear correlation factor, *r*		−0.882	−0.868

[a] The 10^4 k_1 ($M^{-1}\,s^{-1}$) was measured *in vitro* by inhibited autoxidation of styrene (IAS) method [3].
[b] Tocopherol's models.

In addition, the sum of the spin densities on the O_2 and O_3 oxygens in the PCET-TS was in good agreement with the antioxidant activity ($r = -0.868$) (Table 3).

This means that the increased electron densities or spin densities on the O_2 and O_3 oxygens [$(O_2+O_3-O_1)$ charge, $\Delta(O_2+O_3-O_1)$ charge, and (O_2+O_3) spin] in the PCET-TS selectively stabilize the TSs by providing greater binding energy for H^+ transfer.

In the HAT group, linear correlations between the partial atomic charges in the TS and k_1 values were very poor (Table 2). The spin densities on radical oxygens (O_2+O_3) in the HAT-TS were highly negatively correlated

with k_1 ($r = -0.925$), while the spin densities on the ring $[C_{1(\text{bonded to } O_1)} + C_2(ortho) + C_4(para) + C_6(ortho) + O_7(para)]$ (See tocopherol in Fig. 1) in the TS were positively correlated with the rate constant ($r = 0.907$) (Table 3).

For all phenols in the HAT and PCET groups with oxygen bonded in the *para* position of the aromatic ring (O_7), there was relatively high positive correlation between the spin densities on the *para*-oxygen (O_7) in the TS and k_1 ($r = 0.927$), and between the spin densities in the aromatic ring [C_1+C_2(*ortho*)+C_4(*para*)+C_6(*ortho*)+O_7(*para*)] of the TS and k_1 ($r = 0.912$) (Table 4).

The regression curves calculated could be useful for evaluating k_1 for other phenols with a *para*-positioned oxy group (Figs. 3 and 4).

$$k_1 = 9288.662 \cdot (O_7)\text{spin} - 225.044,$$

$$k_1 = 1951.821 \cdot (C_1 + C_2 + C_4 + C_6 + O_7)\text{spin} - 738.253.$$

The HOMO(Ar–OH), SOMO(Ar–O•), and HOMO (Ar–OH) − SOMO(Ar–O•) energies for all the phenols examined were also in relatively good agreement with the k_1 values ($r > 0.722$). The best correlations were found in

Table 4
Spin densities in the TS of phenols with oxygen on *para* position, computed by (U)B3LYP/6-31G (d,p) basis set

Phenols with O_7 (*para*)	k_1[a]	O_7 spin (TS)	(C_1+C_2+C_4+C_6+O_7) spin (TS)
IIIb	570	0.07320	0.57124
IIIa	540	0.08265	0.66052
Ia	380	0.05932	0.60086
(*away*) IIIc	320	0.06964	0.54453
Ib	270	0.05111	0.50890
Ic	180	0.04076	0.51191
DMT	180	0.04223	0.45567
Id	150	0.04474	0.49500
(*away*) γ-tocopherol[b]	140	0.03977	0.45479
(*away*) β-tocopherol[b]	130	0.04568	0.47497
2,6-Dimethyl-4-methoxy-phenol	94	0.02810	0.40148
δ-Tocopherol[b]	44	0.04071	0.40886
2,3,5,6-Tetramethyl-4-methoxy-phenol	39	0.02401	0.38435
Linear correlation factor, *r*		0.927	0.912
Intercept		−225.044	−738.253
Slope		9288.662	1951.821

[a] The 10^4 k_1 (M^{-1} s^{-1}) was measured *in vitro* by inhibited autoxidation of styrene (IAS) method [3].
[b] Tocopherol's models.

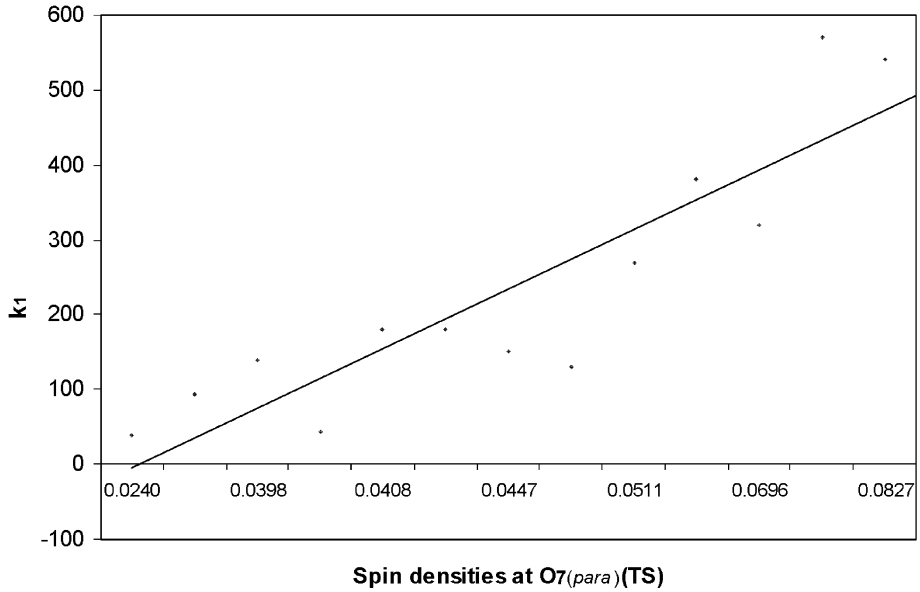

Fig. 3. The (O_7) spin density in the $(CH_3)_3C–O_3–O_2^{\bullet}\cdots H\cdots O_1$–Ar transition structures versus experimental antioxidant activity (k_1 value) for reaction with *tert*-butyl-peroxy radical $(CH_3)_3C–OO^{\bullet}$, and the (C_1+C_2+C_4+C_6+O_7) spin density in the transition structures versus k_1. (a) Values for 10^4 k_1 (M^{-1} s^{-1}) were measured using the inhibited autoxidation of styrene (IAS) method [3].

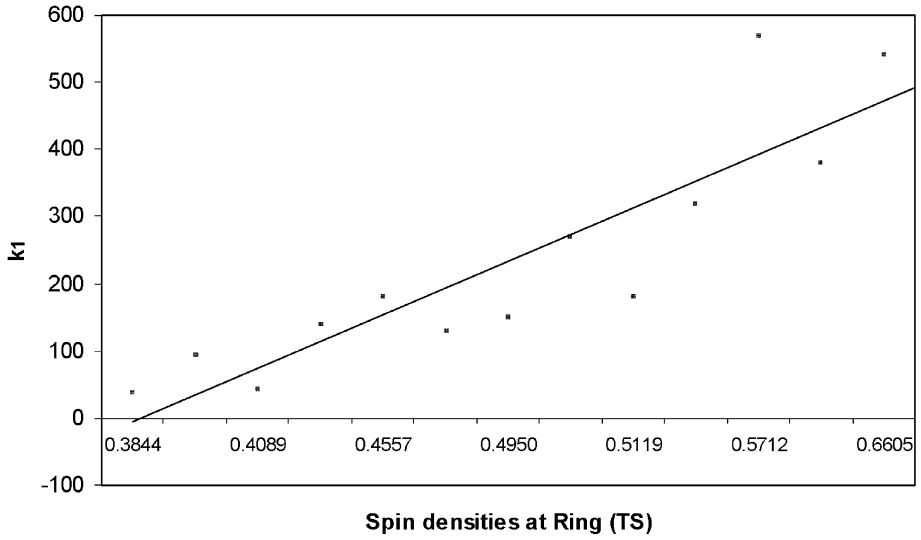

Fig. 4. The (C_1+C_2+C_4+C_6+O_7) spin density in $(CH_3)_3C–O_3–O_2^{\cdot}\cdots H\cdots O_1–Ar$ transition structures versus experimentalental antioxidant activity (k_1 value) for reaction with *tert*-butyl-peroxy radical $(CH_3)_3C–OO^{\cdot}$. (a) The 10^4 k_1 (M^{-1} s^{-1}) was measured by inhibited autoxidation of styrene (IAS) method [3].

Table 5
The BDE $(Ar–OH)^{gas}$, molecular orbitals energies and antioxidant factors (Af) of the phenols, computed by B3LYP/6-31G (d,p) basis set

Compounds	k_1[a]	BDE (kcal/mol)	HOMO (Ar–OH) − SOMO (Ar–O·)	Af
HAT				
(*away*) IIIc	320	75.622	−0.08504	114.955491
Ic	180	75.490	−0.090259	108.3072048
DMT	180	74.578	−0.088537	110.4137253
(*away*) γ-tocopherol[b]	140	76.858	−0.088811	110.0730765
(*away*) β-tocopherol[b]	130	75.313	−0.087857	111.268311
δ-Tocopherol[b]	44	78.907	−0.087877	111.2429874
r with k_1 in HAT group		−0.624	0.536	0.550
PCET				
IIIb	570	72.599	−0.085016	114.9865908
IIIa	540	78.819	−0.084527	115.6518036
Ia	380	73.093	−0.088947	109.9047748
Benzothiopyran derivate	280	75.469	−0.086986	112.3824523
Ib	270	73.936	−0.091197	107.1932191
Id	150	73.757	−0.089716	108.9627268
2,6-Dimethyl-4-methoxy-Ph	94	75.393	−0.089737	108.9372277
2,3,5,6-Tetramethyl-4-methoxy-Ph	39	77.783	−0.093526	104.5238757
2,4,6-Trimethyl-Ph	8.5	78.463	−0.093743	104.2819197
2,6-Dimethyl-Ph	2.5	78.901	−0.096914	100.8698434
phenol			−0.097757	
r with k_1 in PCET group		−0.448	0.888	0.897
Intercept, PCET group				−4095.927
Slope, PCET group				39.803
HAT and PCET				
r with k_1 for all		−0.471	0.746	0.758
Intercept				−3372.071
Slope				32.658

[a] The 10^4 k_1 (M^{-1} s^{-1}) was measured *in vitro* by inhibited autoxidation of styrene (IAS) method [3].
[b] Tocopherol's models.

the PCET group between k_1 and the HOMO(Ar–OH) values ($r = 0.846$) and the HOMO(Ar–OH) − SOMO(Ar–O·) values ($r = 0.888$) (Table 5).

Since the HOMO(Ar–OH), SOMO(Ar–O·), and HOMO(Ar–OH) − SOMO(Ar–O·) values influence the velocity of H-atom transfer in both the HAT and PCET pathways [4,5,7,8], we generated an equation for the antioxidant factor (Af) as the ratio between HOMO-(C_6H_5OH) − SOMO($C_6H_5O^{\cdot}$) values for phenol and HOMO(Ar–OH) − SOMO(Ar–O·) values for the antioxi-

Table 6
The BDE (Ar–OH)^{gas}, molecular orbitals energies and antioxidant factors (Af) of the phenols and their $(CH_3)_3$–CO$^{\bullet}\cdots$H$\cdots$O–Ar transition structures, computed by B3LYP/6-31G (d,p) basis set

Phenols	k_1[a]	BDE (kcal/mol)	HOMO (Ar–OH) − SOMO (Ar–O$^{\bullet}$)	Af
HAT				
α-Tocopherol[b]	420	72.330	−0.08895	109.905
p-tert-Butyl-phenol	190	78.574	−0.09718	100.596
PCET				
2,4,6-Trimethyl-phenol	160	84.395	−0.09420	103.776
p-Chlor-phenol	110	84.941	−0.09693	100.854
3,5-Dichlor-phenol	87	87.948	−0.10266	95.220
Phenol	86	86.135	−0.09776	100.000
p-CF_3-phenol	71	88.035	−0.10583	92.368
Linear correlation factor, *r*		−0.959	0.831	0.859
Intercept				−1695.376
Slope				18.488

[a] The 10^{-7} $k_1/M^{-1}\,s^{-1}$ values were obtained by Laser Flash Photolysis (LFP) with *tert*-butoxyl radical ($(CH_3)_3C$–O$^{\bullet}$) in carbon-tetrachloride as solvent [14].
[b] Tocopherol's model.

dants examined. This antioxidant parameter of the phenols should be an indicator of their total antioxidant activity in reaction with the peroxy radical.

$$\mathrm{Af} = \frac{[\mathrm{HOMO}(C_6H_5\text{–}OH) - \mathrm{SOMO}(C_6H_5\text{–}O^{\bullet})]\cdot 100}{\mathrm{HOMO}(\mathrm{Ar\text{–}OH}) - \mathrm{SOMO}(\mathrm{Ar\text{–}O^{\bullet}})}$$

The best linear correlation was found between k_1 and Af values ($r = 0.897$) in the PCET group. The calculated regression curve $k_1 = 39.803\cdot\mathrm{Af} - 4095.927$ is useful for k_1 evaluation of other phenolic antioxidants in reaction with the peroxy radical via a dominant PCET pathway (Table 5). Also, for all phenols analyzed there was relatively good linear correlation between k_1 and Af values ($r = 0.758$).

Furthermore, the theoretical method developed was used to evaluate reactions between other phenolic antioxidants and the *tert*-butyloxy radical $(CH_3)_3$–CO$^{\bullet}$ [14]. The experimental 10^{-7} k_1 ($M^{-1}\,s^{-1}$) values were obtained by laser flash photolysis (LFP) in carbon tetrachloride (CCl_4) as solvent [14].

The dominant H atom transfer mechanism was determined according to SOMO conformations in the TSs and charge changes on the hydrogen in the $(CH_3)_3$–COO$^{\bullet}\cdots$**H**$\cdots$O–Ar TS compared to the parent phenol. In fact, a decrease in the H-atom charge in the TS compared to the phenol indicated a dominant H$^{\bullet}$ transfer (HAT), while an increase in the H-atom charge in the TS compared to the parent phenol signified a dominant H^+ transfer (PCET) [4].

For all phenols examined in the HAT and PCET groups, there was good linear correlation between the experimental k_1 rates [14] and calculated BDE(Ar–OH)^{gas} ($r = -0.959$), Af values ($r = 0.859$), and SOMO(Ar–O$^{\bullet}$) ($r = 0.855$) and HOMO(Ar–OH) energies ($r = 0.854$) (Table 6). Thus, it was concluded that the BDE(Ar–OH)^{gas}, the antioxidant factor, and the calculated regression curve ($k_1 = 18.488\cdot\mathrm{Af} - 1695.376$) are useful in predicting phenol reactivity with the alkoxyl radical (Table 6).

4. Discussion

The theoretical method developed for the examination of phenolic antioxidants involves determination of the dominant H-atom transfer mechanism according to the ΔH(TS) and SOMO(TS) conformation, as well as evaluation of charge changes [O_2+O_3−O_1, Δ(O_2+O_3−O_1)], spin densities (O_2+O_3, O_7, C_1+C_2+C_4+C_6+O_7), BDE(Ar–OH)^{gas}, and HOMO/SOMO energies inside the PCET and HAT groups. Molecular parameters with the strongest influence on the phenols activities in each group were selected and corresponding regression equations were calculated.

In the first part of the study were examined transition structures of *tert*-butyl-peroxy radical with selected phenolic antioxidants [$(CH_3)_3$COO$^{\bullet}\cdots$H$\cdots$O–Ar] [3].

For the PCET pathway, the increased electron densities or spin densities on the O_2 and O_3 oxygens [(O_2+O_3−O_1) charge, Δ(O_2+O_3−O_1) charge, and (O_2+O_3) spin] in the PCET-TS can selectively stabilize the TSs by providing greater binding energy for the H^+ transfer.

For the HAT reactions, the higher spin densities on the radical oxygens (O_2+O_3) and the lower delocalization of spin in the ring [C_1+C_2(*ortho*)+C_4(*para*)+C_6(*ortho*)+O_7(*para*)] of the HAT-TS lead to a decrease in antioxidant activity.

In the TS of phenols containing O_7(*para*), the spin densities on O_7(*para*) and on the ring were correlated well with k_1 ($r > 0.91$). Thus, the total antioxidant activity (k_1) for the phenols can be calculated from the equations $k_1 = 9288.662\cdot(O_7)\mathrm{spin} - 225.044$ and $k_1 = 1951.821\cdot(C_1+C_2+C_4+C_6+O_7)\mathrm{spin} - 738.253$.

Also, for all phenols analyzed there was relatively good linear correlation between k_1 and Af values ($r = 0.758$). The corresponding regression curve, $k_1 = 32.658\cdot\mathrm{Af} - 3372.071$, could be applied for estimation of the total antioxidative activity of other phenols in reaction with the per-

oxy radical before selection of the dominant H-atom transfer mechanism (Table 5).

The correlations calculated between the selected parameters and the k_1 values [3] should be accepted as relatively high, because the phenols examined are very different in structure and activity (10^4 $k_1 = 2.5$–570 M^{-1} s^{-1}).

Since the reactivity of phenols with the alkylperoxy radical does not depend strongly on the structure of the radical [18], the procedure presented can be used to estimate phenol reactivity with any alkylperoxy radical R–O–O$^{\cdot}$ [3,18].

The theoretical method used selected PCET as the dominant mechanism for α-tocopherol (Ia) reaction with the *tert*-butyl-peroxy radical, and HAT as the main pathway for α-tocopherol (Ia) reaction with the *tert*-butyloxy radical (Tables 2, 3 and 6).

The different H-atom transfer mechanisms of α-tocopherol (Ia) in reaction with oxygen-centered radicals indicate that investigation of TSs between phenolic antioxidants and specific radicals is necessary as a first step in investigating their antioxidative properties.

5. Conclusion

A dominant H atom transfer mechanism in the reaction of phenols with certain types of oxygen-centered radicals was selected by examining the conformations, singly occupied molecular orbitals (SOMOs), charge separation and spin density in optimized transition structures such as $(CH_3)_3$–C–O_3–$O_2^{\cdot}\cdots H\cdots O_1$–Ar and $(CH_3)_3$–C–$O_2^{\cdot}\cdots H\cdots O_1$–Ar. The change in charge on the hydrogen (ΔH) and the SOMO conformations in the TSs were used as criteria for determining the dominant H-atom transfer mechanism. Increased electron density on the O_2 and O_3 oxygens in the PCET-TS gives greater binding energy for H^+ transfer, while the low spin densities on the radical oxygens (O_2+O_3) and the high spin densities on the ring in the HAT-TS facilitate the H atom transfer. In the TS of phenols containing O_7 (*para*) in the structure, the high spin densities on O_7 (*para*) and on the ring increase rate of the reaction between the phenols and the radicals (k_1).

This study can help in understanding the structural features that contribute to the action of a phenol, and hence can be used to predict the main pathway and activity of novel phenolic antioxidants thereby designing compounds with enhanced activity.

Using the procedure outlined in this paper we are currently attempting to examine reactions between phenols and other types of free radicals.

Appendix A. Supplementary data

Supplementary data associated with this article can be found, in the online version, at doi:10.1016/j.theochem.2006.07.017.

References

[1] O.I. Aruoma, A.M. Murcia, J. Butler, B. Halliwell, J. Agric. Food Chem. 1880 (1993) 41.
[2] B. Halliwell, R. Asechbach, J. Iloliger, O. Aruoma, J. Food Chem. Toxicol. 601 (1995) 33.
[3] G.W. Burton, T. Doba, E.J. Gabe, L. Hughes, F.L. Lee, L. Prasad, K. Ingold, J. Am. Chem. Soc. 7053 (1985) 107.
[4] J.M. Mayer, D.A. Hrovat, J.L. Thomas, W.T. Borden, J. Am. Chem. Soc. 11142 (2002) 124.
[5] G.W. Burton, K. Ingold, Acc. Chem. Res. 194 (1986) 19.
[6] P. Mulder, H.G. Korth, K. Ingold, Helv. Chim. Acta 370 (2005) 88.
[7] G.A. DiLabio, D.A. Pratt, A.D. LoFaro, J.S. Wright, J. Phys. Chem. A 1653 (1999) 103.
[8] C. Guo Zhang, J.A. Nichols, D.A. Dixon, J. Phys. Chem. A 4184 (2003) 107.
[9] L.J.J. Laarhoven, P. Mulder, D.D.M. Wayner, Acc. Chem. Res. 342 (1999) 32.
[10] G.F. Pedulli, M. Lucarini, P. Pedrielli, in: F. Minisci (Ed.), Free Radicals in Biology and Enviroment, Kluwer Academic Publishers., Dordrecht, The Netherelands, 1997, p. 169.
[11] M.I. de Heer, H.G. Korth, P. Mulder, J. Org. Chem. 6969 (1999) 64.
[12] M. Lukarini, V. Magnaini, G.F. Pedulli, J. Org. Chem. 928 (2002) 67.
[13] D.V. Avila, K. Ingold, J. Lusztyk, J. Am. Chem. Soc. 2929 (1995) 117.
[14] D.W. Snelgrove, J. Lusztyk, J.T. Banks, P. Mulder, K. Ingold, J. Am. Chem. Soc. 469 (2001) 123.
[15] M.H. Abraham, P.L. Grellier, D.V. Prior, P.P. Duce, J.J. Morris, P.J. Taylor, J. Chem. Soc. Perkin Trans. 2 699 (1989) 6.
[16] M.H. Abraham, P.L. Grellier, D.V. Prior, J.J. Morris, P.J. Taylor, J. Chem. Soc. Perkin Trans. 2 521 (1990) 4.
[17] M. Guerra, R. Amorati, G.F. Pedulli, J. Org. Chem. 5460 (2004) 69.
[18] J.H.B. Cheing, E. Furimsky, J.A. Howard, Can. J. Chem. (1974) 52.
[19] J.E. Packer, T.F. Slater, R.L. Wilson, Nature (London) 737 (1979) 278.
[20] J.J.P. Stewart, MOPAC 2000 Version 7.0.0, Fujitsu Limited, Tokyo, Japan.
[21] M.J. Frisch, G.W. Trucks, H.B. Schlegel, G.E. Scuseria, M.A. Robb, J.R. Cheeseman, V.G. Zakrzewski, J.A. Montgomery Jr., R.E. Stratmann, J.C. Burant, S. Dapprich, J.M. Millam, A.D. Daniels, K.N. Kudin, M.C. Strain, O. Farkas, J. Tomasi, V. Barone, M. Cossi, R. Cammi, B. Mennucci, C. Pomelli, C. Adamo, S. Clifford, J. Ochterski, G.A. Petersson, P.Y. Ayala, Q. Cui, K. Morokuma, D.K. Malick, A.D. Rabuck, K. Raghavachari, J.B. Foresman, J. Cioslowski, J.V. Ortiz, A.G. Baboul, B.B. Stefanov, G. Liu, A. Liashenko, P. Piskorz, I. Komaromi, R. Gomperts, R.L. Martin, D.J. Fox, T. Keith, M.A. Al-Laham, C.Y. Peng, A. Nanayakkara, C. Gonzalez, M. Challacombe, P.M.W. Gill, B.G. Johnson, W. Chen, M.W. Wong, J.L. Andres, M. Head-Gordon, E.S. Replogle, J.A. Pople, Gaussian 98 (Revision A.7), Gaussian, Inc., Pittsburgh PA, 1998.
[22] A.D. Becke, J. Chem. Phys. 5648 (1993) 98.
[23] C. Lee, W. Yang, R.G. Parr. Phys. Rev. B. 785 (1988) 37.
[24] G.A. DiLabio, D.A. Pratt, J.S. Wright, Chem. Phys. Lett. 215 (1999) 311.
[25] T. Fox, P.A. Kollman, J. Phys. Chem. 2950 (1996) 100.
[26] G.A. DiLabio, D.A. Pratt, J.S. Wright, Chem. Phys. Lett. 181 (1998) 297.
[27] J.S. Wright, J.D. Carpenter, D.J. McKay, K.U. Ingold, J. Am. Chem. Soc. 4245 (1997) 119.
[28] J.S. Wright, E.R. Johnson, G.A. DiLabio, J. Am. Chem. Soc. 1173 (2001) 123.
[29] M. Dewar, W. Thiel, J. Am. Chem. Soc. 2338 (1977) 99.
[30] M.J.S. Dewar, E.G. Zoebish, E.F. Healy, J.J.P. Stewart, J. Am. Chem. Soc. 3902 (1985) 107.
[31] D.M. Chipman, R. Liu, X. Zhou, P. Pulau, J. Chem. Phys. 5023 (1994) 100.

[32] Y. Qin, R.A. Wheeler, J. Chem. Phys. 1689 (1995) 102.
[33] B.J.C. Costa Cabrol, R.G.B. Fonseca, J.A.M. Simoes, Chem. Phys. Lett. 436 (1996) 258.
[34] N.W. Larsen, J. Mol. Struct. 175 (1979) 51.
[35] M.J.S. Dewar, E.G. Zoebisch, E.F. Healy, J.J.P. Stewart, J. Am. Chem. Soc. 3902 (1985) 107.
[36] D.R. Lide (Ed.), CRC, Hand book of Chemistry and Physics, CRC Press, Boca Raton FL, 1994, pp. 9–37.
[37] H.D. Bist, J.C.D. Brand, D.R. Williams, J. Mol. Spectosc. 402 (1967) 24.
[38] C.M. Breneman, K.B. Wiberg, J. Comput. Chem. 361 (1990) 11.
[39] M. Lucarini, G.F. Pedulli, M. Cipollone, J. Org. Chem. 5063 (1994) 59.
[40] J. Lind, X. Shen, T.E. Eriksen, G. Merenyi, J. Am. Chem. Soc. 479 (1990) 112.
[41] D.D.M. Wayner, E. Lusztyk, K. Ingold, P. Mulder, J. Org. Chem. 6430 (1996) 61.
[42] G.A. DiLabio, D.A. Pratt, J.S. Wright, J. Org. Chem. 2195 (2000) 65.
[43] W.J. Hehre, L. Radom, P.v.R. Schleyer, J.A. Pople, Ab Initio Molecular Orbital Theory, Wiley, 1986.